JOURNAL OF GUIDANCE, CONTROL, AND DYNAMICS
Vol. 32, No. 4, July–August 2009

Approach and Landing Flight Evaluation of Smart-Cue and Smart-Gain Concepts

David H. Klyde* and Chi-Ying Liang†
Systems Technology, Inc., Hawthorne, California 90250

DOI: 10.2514/1.43157

The smart-cue and smart-gain concepts were developed as a means to alleviate pilot–vehicle-system loss of control in the presence of control surface actuator rate limiting. Both concepts exploit the measure of dynamic distortion, that is, the difference between the actual and an ideal aircraft control system response. The concept of dynamic distortion has significantly evolved in work conducted by Systems Technology, Inc., during a two-phase program sponsored by NASA Dryden Flight Research Center. In this work, the distortion of interest results from control surface rate limiting and is quantified by the surface position error, whereas the distortion metric is the position lag. A force feedback cue (the constraining function) and/or a command path gain reduction are created when the position error exceeds the position lag (the alerting function). This paper examines the approach and landing flight-test evaluations conducted using the Calspan Corporation Learjet II In-Flight Simulator. Three test pilots evaluated several smart-cue and smart-gain implementations while performing the precision offset landing task. One of the pilots flew on a calm air day, whereas the other two flew on days with moderate turbulence and significant crosswinds. The clear performance enhancer for all three pilots was the smart-gain, however, the best results for the two pilots who flew under adverse conditions were obtained for the configuration that featured both the smart-cue and smart-gain active. This configuration eliminated the undesirable motions that were encountered in the final centerline correction when only the smart-gain was active.

I. Introduction

BEFORE the Wright brothers, both aeronautical theorists and practical engineers focused on aircraft that were stable. This made sense because many of the experimental efforts used aircraft models that were not controlled and hence were intrinsically designed to be very stable. But these craft did not turn very well and, as their stability was generally with respect to the air mass, they were quite sensitive to gusts. The Wrights changed this, with the realization that controllable flight, even at the price of aircraft stability, was essential. They reasoned, based at least in part on their experience with bicycles, that stability around desirable flight paths was indeed central, but that the secret to this (stated in modern terms) was to have a system comprising the pilot–vehicle combination that was controllable and stable. Of course, the Wrights' efforts worked out, but ever since there have been several generations of different problems in pilot–vehicle-system control, some of which persist today, more than 100 years after the first powered flight. Unfavorable aircraft–pilot couplings, including pilot-induced oscillations (PIOs), have been particularly ubiquitous although not, by any means, the only variety.

At present, the aircraft flying qualities community has sufficient understanding of pilot–vehicle systems in general to make the case that some effective vehicle dynamic characteristics can be considered to be either ideal or good enough. Departures from these nominally ideal properties can then be defined as distortions that may underlie pilot–vehicle-system problems. A common example is control surface rate limiting, where deviation from desirable values has been shown to lead to PIOs in some circumstances. Another example is misrigging of control system elements, such as mechanical maladjustments leading to control system backlash or excessive hysteresis. The common theme is that the actual manual flight control system is in some way deviating from an ideal system. The pilot is expecting one type of response, but the actual system is behaving differently because of the distortion. Within this general context, Ralph A'Harrah of NASA Headquarters (now retired) proposed the Loss of Control Inhibition System (LOCIS)[‡] wherein distortions are detected and appropriate cues are then introduced to the pilot by way of compensation. It was recognized at the time that this was still a general concept that had yet to be made concrete or specific. It served as a motivation for the work reported herein to attempt to quantify such conceptual terms as "distortions" and "idealized systems" as innovative and unifying principles underlying the development of corrective measures in the form of controller cues.

To advance this generalized theme, concrete examples were needed. As part of a NASA Phase II Small Business Innovation Research effort, Systems Technology, Inc. (STI) examined one critical distortion, that involving control surface rate limiting as a factor in category II PIO [1] and loss of control, and evolved and successfully demonstrated some conceivable alleviation means (herein referred to as the smart-cue and smart-gain). Because rate limiting has been a contributing if not causal factor in all of the severe PIO loss of control events involving modern fly-by-wire aircraft, this distortion remained the focus for the Phase II flight-test program. This paper presents the approach and landing results from a flight-test evaluation of the smart-cue and smart-gain concepts. A companion paper examines the dynamic distortion concept and the evolution of the smart-cue and smart-gain [2].

II. Learjet In-Flight Simulator Description

A. Overview

The Calspan Corporation variable stability Learjets are modified Learjet Model-24 and 25 aircraft (the Model-25 shown in Fig. 1 was used in this program). The Learjets provide 3-degree-of-freedom (3-DOF) in-flight simulation capabilities for advanced stability, control, and flying qualities demonstrations and research [3]. They are also used to test/demonstrate advanced flight control systems concepts.

Presented as Paper 6210 at the AIAA Atmospheric Flight Mechanics Conference and Exhibit, Honolulu, HI, 18–21 August 2008; received 9 January 2009; revision received 28 February 2009; accepted for publication 2 March 2009. Copyright © 2009 by Systems Technology, Inc. Published by the American Institute of Aeronautics and Astronautics, Inc., with permission. Copies of this paper may be made for personal or internal use, on condition that the copier pay the $10.00 per-copy fee to the Copyright Clearance Center, Inc., 222 Rosewood Drive, Danvers, MA 01923; include the code 0731-5090/09 $10.00 in correspondence with the CCC.

*Technical Director. AIAA Associate Fellow.
†Senior Research Engineer.

‡The A'Harrah LOCIS concept was recently awarded two U.S. Patents (#7,285,932 and #7,285,933).

Fig. 1 Variable stability Learjet 25 (Calspan photo).

The three aircraft are used in these capacities to support flight-test training of test pilots and flight-test engineers around the world, as well as support new aircraft development programs.

As described in [3], the right seats of the Learjets have been extensively modified to serve as the evaluation pilot (EP) crew station. The normal Learjet wheel/column has been removed. It is replaced with one of three experimental controllers: 1) center stick, 2) side stick, and 3) wheel/column. Each of these two axis control inceptors has programmable variable feel capability, allowing simulation and evaluation of a wide range of characteristics. The Learjet's aircraft rudder pedals have also been replaced with variable feel capability. Electrohydraulic servo actuators drive the aircraft's primary control surfaces in response to pilot inputs and the signals from the variable stability system (VSS). The safety pilot (SP), whose controllers remain mechanically connected to the Learjet control surfaces, via cables, occupies the left seat. Figure 2 shows the modified aircraft configuration with the incorporated VSS components.

B. Variable Stability System Description

As described in [3], in-flight simulation is performed using control laws hosted in the VSS computers. These computers include the original hybrid digital/analog units and a fully digital unit. Each VSS computer system is composed of two independent subsystems. The first, the variable feel system, provides the EP with tactile force cues from the pitch/roll controller and rudder pedals, that is, gradients, displacements, and nonlinearities such as breakout. The second hosts the control laws, which augment the Learjet dynamics to represent those of the vehicle to be simulated.

The all-digital unit consists of several digital signal processors (DSPs) installed in a PC. The DSPs compute and control the feel system, input/output management, and augmentation control law algorithms. The host PC allows simulation control, passing data to and from the DSPs, data recording, and real-time plotting. The DSPs can be programmed directly or symbolically using MATLAB Simulink. This makes the VSS a useful tool for rapid prototyping and allows quick turnaround of desired system changes. The architecture of the analog sensor conditioning electronics and of the VSS computing equipment allows easy interface with sensors, augmentation control laws, feel systems, and cockpit displays (including the programmable head-down display shown in Fig. 2).

The Learjets are equipped with onboard systems for recording test data. Data acquisition is controlled by the PC host computer interface at the test engineer console or by the SP via a handheld keypad. Up to 512 channels of digital data may be recorded directly from the DSP computers and stored on removable flash memory. Selected parameters may be directed to the test engineer's computer displays for real-time monitoring. Audio and video information (from cameras, displays, and crew voices) is also recorded onboard using a DVD recorder. The aircraft also has provisions for telemetry transmission of data, audio, and video signals.

III. Flight-Test Configuration

A. Lateral Axis Feel System

The lateral feel system dynamics for the stick are modeled as a second-order system with nonlinearities. All parameters such as breakout, force gradients, and friction levels are fully configurable and variable in flight. The evaluation pilot applies a force on the stick which is measured and sent into the dynamic stick model to obtain the model stick position from the force. This position is then put through an inverse dynamic model of the physical stick and servo dynamics to obtain a command for the feel system servo that drives it to the position of the model.

Key feel system elements are shown in the Fig. 3 block diagram. These include the dynamic characteristics of the control loader and the control system gearing. A summary of the baseline feel system characteristics used in this flight-test program is provided in Table 1. As described previously, these characteristics can be easily varied from this baseline. The steady-state stick force characteristics are shown in the right side panel of Table 1 and the Bode frequency response is shown in Fig. 4. The steady-state characteristics were

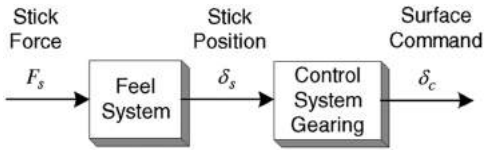

Fig. 3 Feel system elements.

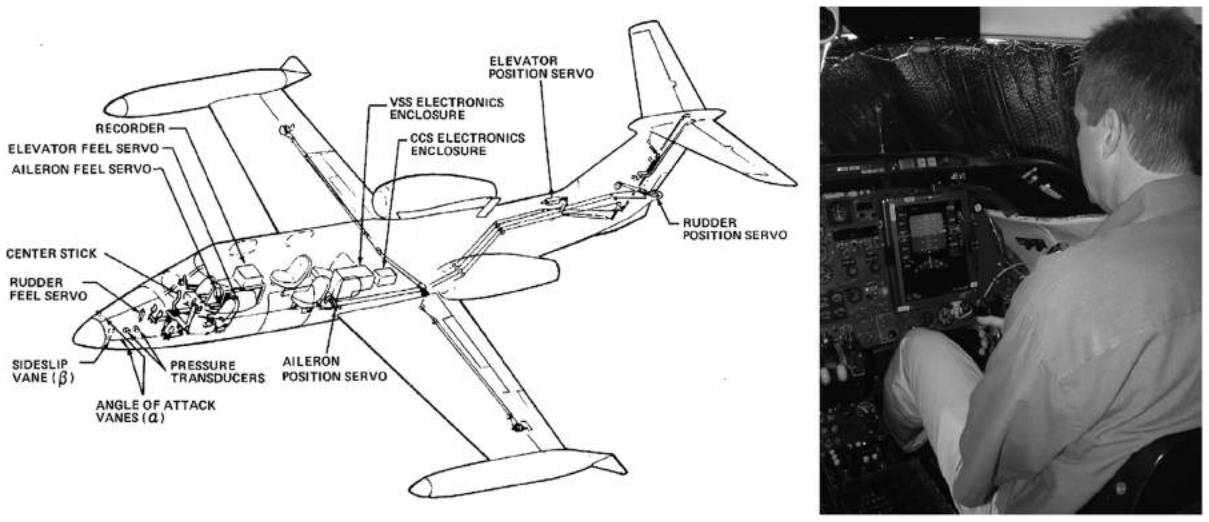

Fig. 2 Learjet configuration layout and cockpit in ground simulation mode with programmable head-down display [3].

Table 1 Lateral feel system characteristics

Parameter	Value
Spring gradient, lb/in	5.65
Damping, lb · s/in.	0.395
Natural frequency, rad/s	20
Damping ratio	0.7
Inertia, lb · s^2/in.	0.0141
Breakout, lb	0.25
Travel, in.	±3.1
Control system gearing, deg/in.	−12.3

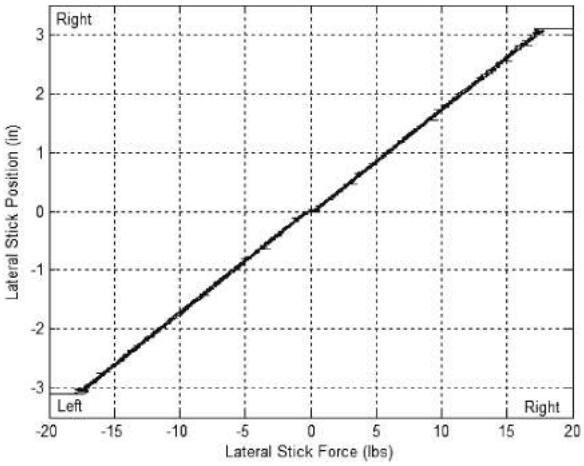

Table 2 Lateral axis flight control system parameters

Flight control system element	Form	Parameter values
Software rate limit, deg /s	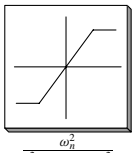	$V_L = 25, 30, 150$ (baseline)
Surface actuator	$\frac{\omega_n^2}{s^2+2\zeta\omega_n s+\omega_n^2}$	$\omega_n = 44$ rad/s; $\zeta = 0.7$
Surface position limits	$\delta_{a_{\max}}$	±40 deg

generated from the EP station of Learjet 2 while operating in ground simulation mode. The frequency responses, on the other hand, were generated in flight. The lines on the Bode plot represent a transfer function fit using the Table 1 parameters (solid line for magnitude and dashed line for phase), whereas the symbols represent data collected from a pilot-generated frequency sweep (circles for magnitude and squares for phase). The resulting transfer function[§] is included in the figure.

B. Lateral Axis Flight Control System

The key lateral axis control system elements downstream of the feel system are identified in Fig. 5. These elements include the software rate limiter, surface actuator, and surface position limits. The software rate limiter is the key dynamic distortion inducing element [2] that was routinely used in the smart-cue/smart-gain evaluation. The control surface actuator dynamics and surface position limits replicate those found on the Calspan variable stability Learjet. Parameters for the control system elements are defined in Table 2.

C. Approach and Landing Aircraft Configuration

The evaluation task for the approach and landing flight condition was the precision offset landing. Because of the limited number of available flight hours, smart-cue/smart-gain evaluations focused on the lateral axis. The longitudinal configuration was representative of a standard Learjet 25. The nominal approach speed was 140 kt with gear down and flaps set to 20 deg. The approach speed was reduced at the discretion of the safety pilot as the fuel load decreased.

The baseline roll approach and landing configuration had characteristics similar to a nominal Learjet 25 with yaw damper engaged. The configuration is susceptible to PIOs in the presence of significant rate limiting. A frequency response for the baseline roll configuration obtained from a checkout flight-pilot-generated frequency sweep is shown in Fig. 6. Once again, the lines on the plot represent a transfer function fit using the known model dynamics where only the effective gain and delay were adjusted (solid line for magnitude and dashed line for phase), whereas the symbols represent data collected in flight (circles for magnitude and squares for phase). The resulting roll rate p to lateral stick force Fas transfer function is as follows:

$$\frac{p}{Fas} = \frac{4.082e6(0)[0.335, 1.103]}{(-5.49e-3)[0.249, 1.25](1.324)[0.7, 20][0.7, 44]} e^{-0.125s}$$

IV. Flight-Test Description

A. Test Procedures

The flight-test evaluations were conducted as a formal handling qualities evaluation. To this end, the following procedures were followed:

1) Evaluation pilots were familiarized with the evaluation tasks using "good" aircraft configurations (i.e., the baseline configuration described earlier) with no distortion inducing nonlinearities [2] present.

2) An appropriate level of familiarity was met when the pilot could routinely achieve desired performance with the selected evaluation task when presented the good configuration.

3) Degraded configurations were then presented to the pilot to evaluate before any force feedback smart-cues and command path smart-gains were introduced.

4) For the approach and landing evaluations, the smart-gain was introduced first in isolation and then in combination with the smart-cues.

[§]The shorthand form of displaying transfer function is defined by $a(s+b)[s^2+2\zeta\omega s+\omega^2] = a(b)[\zeta, \omega]$.

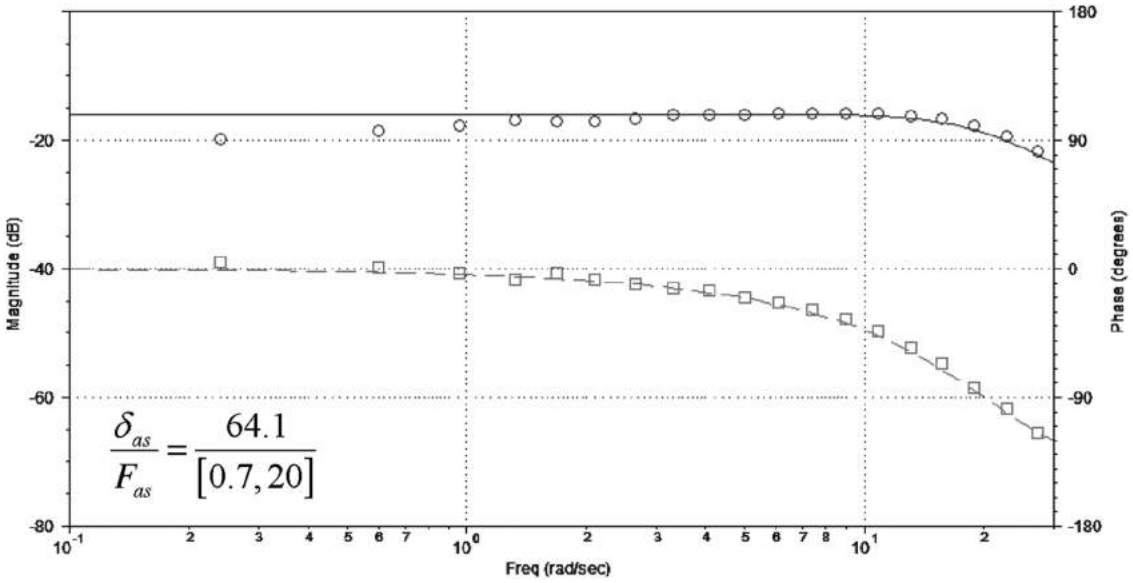

Fig. 4 Longitudinal feel system frequency response identification.

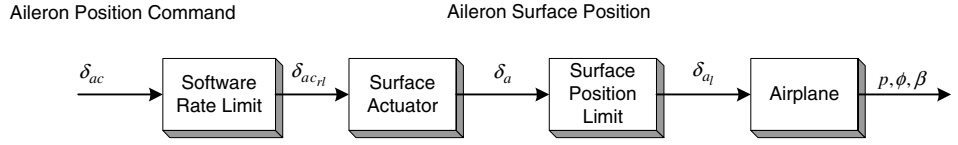

Fig. 5 Lateral axis control system elements.

5) Two smart-cues were introduced: a frictionlike force cue and a combined friction and spring gradient force cue. The pilot evaluated each cue individually.

6) When conducting a formal evaluation, the pilot was asked to perform the selected evaluation task as many times as necessary (within reason) before providing pilot comments and ratings.

7) Cooper–Harper handling qualities ratings [4] and PIO tendency ratings [4,5] were collected. Evaluation pilots were encouraged to talk through the rating scale decision trees as a means of extracting additional commentary.

8) A detailed run log was taken and video with a view from over the evaluation pilot's shoulder was recorded including audio commentary.

The purpose of the smart-cue and smart-gain is to provide protection from the flying qualities cliffs associated with dynamic distortion. The cue thus serves two functions: alerting and constraining. The former annunciates the presence of a potential handling qualities cliff, whereas the latter suppresses inputs that will lead to an encounter with that cliff. The purpose of the evaluation task used here was to simulate the types of closed-loop control scenarios that have produced such cliffs in operational and flight-test aircraft. Although task performance was important, the real evaluation was to determine if the smart-cue and smart-gain could serve as a protection from these cliffs. To this end, some sacrifice in task performance was anticipated when the cues were encountered.

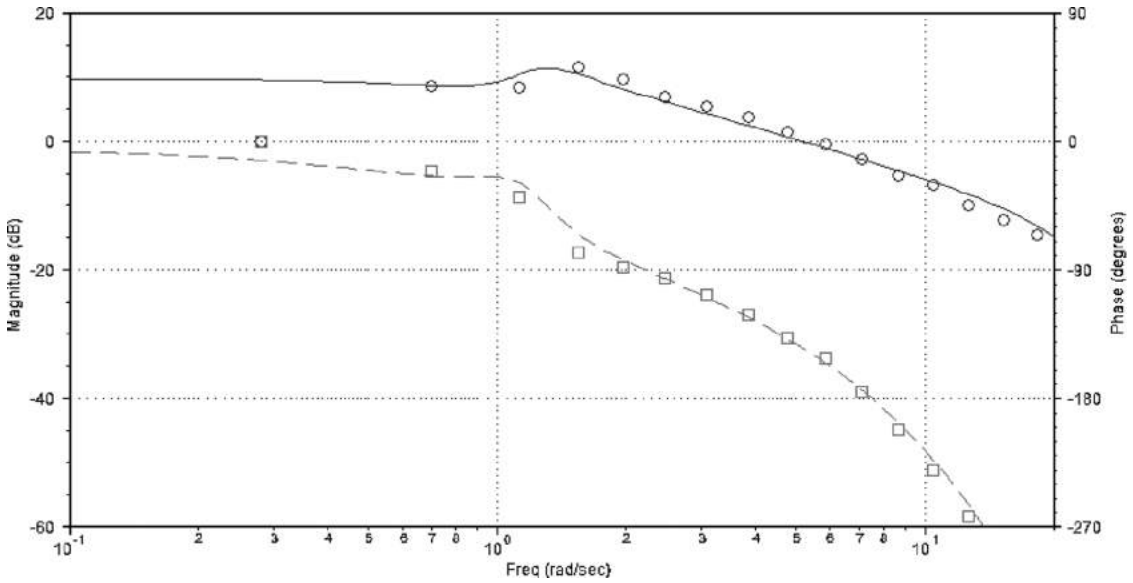

Fig. 6 Bode frequency response of the baseline roll axis approach and landing configuration.

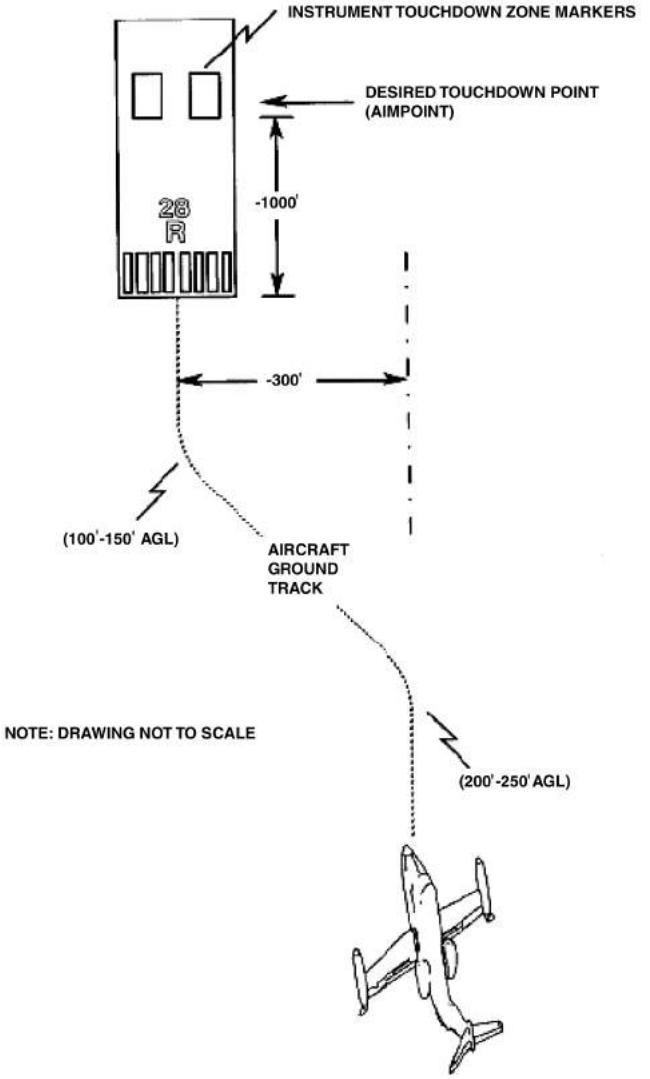

Fig. 7 Offset approach to Niagara Falls Airport [7].

B. Precision Offset Landing Task Description

All of the approach and landing evaluations were made at Niagara Falls Airport. The crew for the checkout and evaluation flights consisted of a Calspan safety pilot, an evaluation pilot, a Calspan flight-test engineer, and the STI flight-test conductor. The evaluation task was the precision offset landing task described next.

Task Objectives

1) Evaluate the ability to precisely control horizontal and vertical flight path and airspeed.

2) Evaluate the ability to precisely control sink rate and attitude in the flare.

3) Evaluate tendency for nose bobble or PIOs.

4) Evaluate control sensitivity and harmony in landing.

Task Description

The offset landing task consists of a visual approach during which the evaluation pilot aligns the aircraft approximately 300 ft off the runway centerline (see Fig. 7). At 150–200 ft above the ground, the EP corrects back to the centerline and attempts to touch down within the desired parameters. The decision to correct is made by the SP. Offsets to the left or right can be used interchangeably; however, the direction of offset may often be dictated by the desire to turn away from civilian aircraft waiting in the hold short area. Typically, offsets were made to the right in this flight-test program to take advantage of the drainage ditch visual cue located approximately 250–300 ft to the right of runway 28R (see Fig. 8). Each landing was treated as a "must land" situation to ensure a high pilot gain.

During a typical landing pattern evaluation, the SP configures the aircraft for landing, selects the proper flight control experiment, and engages the VSS while on downwind. The EP begins the evaluation on base turn and lines up on final for the offset landing. The EP initiates the offset correction on his or her own or based on radar altitude calls from the SP. A precise flared landing is attempted using the instrument landing markers as the desired touchdown point. These markers are located 1000 ft from the threshold. Upon touchdown, the SP takes control of the airplane and performs the takeoff and turn to downwind, while the EP provides comments and handling qualities ratings for that configuration. The head-down display used for the task is shown in Fig. 2.

Desired performance requirements were as follows: 1) approach airspeed maintained within ± 5 kt, 2) touchdown within 5 ft of

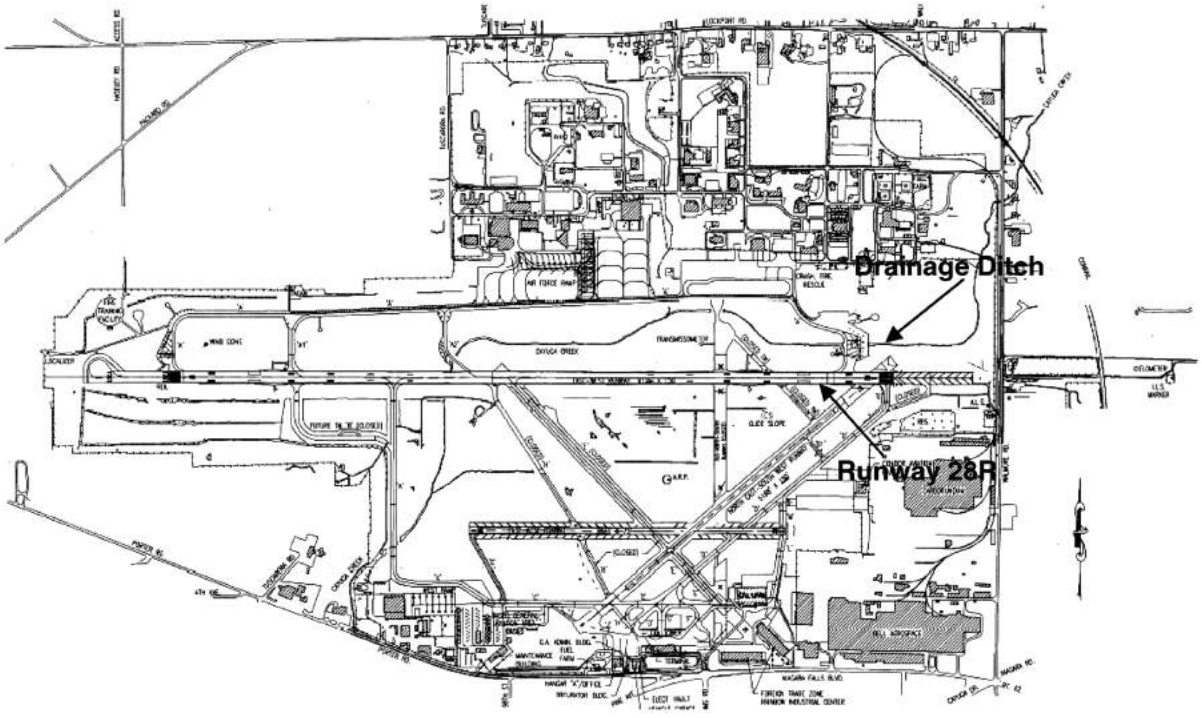

Fig. 8 Layout of Niagara Falls Airport.

centerline (main wheels on centerline), 3) touchdown within ±250 ft of aimpoint, 4) sink rate–smooth touchdown, and 5) no PIO.

Adequate performance requirements were as follows: 1) approach airspeed maintained within −5 KT/ + 10 KT, 2) touchdown within 25 ft of centerline, 3) touchdown within ±500 ft of aimpoint, and 4) no PIO.

V. Flight-Test Results

A. Overview

Seven test pilots participated in this program. Pilots 1 and 2 served as safety pilots and did not conduct formal evaluations. All of the evaluation pilots were graduates of either the U.S. Air Force or U.S. Navy test pilot schools. Approach and landing flights were conducted with three of the five evaluation pilots. Pilots 3 and 4 did not conduct approach and landing evaluations due to poor weather conditions. Pilot 5 flew his approaches in nearly ideal conditions: calm air and good visibility. Under these conditions, the roll axis software rate limit needed to be reduced from 30 to 25 deg/s, so that the handling qualities cliff could be properly exposed. Pilots 6 and 7, on the other hand, conducted their approach and landing evaluations in the presence of moderate turbulence and crosswinds. Thus, no changes to the experimental procedures were required for these flights.

In the following discussion, three example runs were selected for each pilot: 1) the rate-limited configuration, 2) the rate-limited configuration with smart-gain, and 3) the rate-limited configuration with smart-gain and smart-cue. Throughout the remainder of this section, the following symbols are used: RL (rate limit), G (smart-gain), F (friction smart-cue), and C (combined gradient plus friction smart-cue). The number associated with the RL symbol is the magnitude of the rate limit in degrees per second, whereas the number associated with the smart-gain and smart-cue symbol refers to particular configurations.

B. Pilot Ratings and Comments

For the roll axis approach and landing evaluations, the clear performance enhancer was the smart-gain. The addition of the smart-cue, however, was an important and necessary performance benefit for two of the three pilots. For these pilots, the flights took place on a day with significant crosswinds and turbulent air that added work load to the precision offset landing task. In these cases, the same gain reduction and feedback cue produced the best results for both pilots. The other pilot flew on a calm air day, which allowed him to use smoother pilot inputs and a lower gain technique. In this environment, the smart-gain alone did much of the work and only small smart-cue forces that may have been imperceptible to the pilot were ever present.

Cooper–Harper pilot handling qualities ratings (HQR) and pilot-induced oscillation tendency ratings (PIOR) were collected to compliment specific commentary in the qualitative assessment of the various configurations presented to the pilots. Summary PIOR versus HQR plots for each pilot are given in Fig. 9. As mentioned earlier, a slightly lower rate limit was required for the evaluations of pilot 5 due to the calm air day combined with a lower gain piloting technique. Nonetheless, all three pilots gave the rate-limited configuration level 3 pilot ratings (i.e., HQR $\geq$ 7) with observed PIO tendencies (i.e., PIOR $\geq$ 4). For pilot 5, the G1 smart-gain made the greatest impact on his ratings, to the extent that desired performance was attained. A more modest improvement was observed for pilots 6 and 7. The G2 smart-gain configuration, defined by a less aggressive command path gain reduction compared to the G1 configuration, did not produce improved results. The presence of the smart-cues was not a factor in the qualitative evaluations of pilot 5. For pilots 6 and 7, both of whom conducted their evaluations in moderate turbulence and crosswinds, the strongly preferred configuration was G1/C2. This smart-cue/smart-gain combination gave consistent performance (HQR 4/PIOR 2) over repeated runs for both pilots. A summary of pilot comments for the example run evaluations shown in the next section is provided in Table 3.

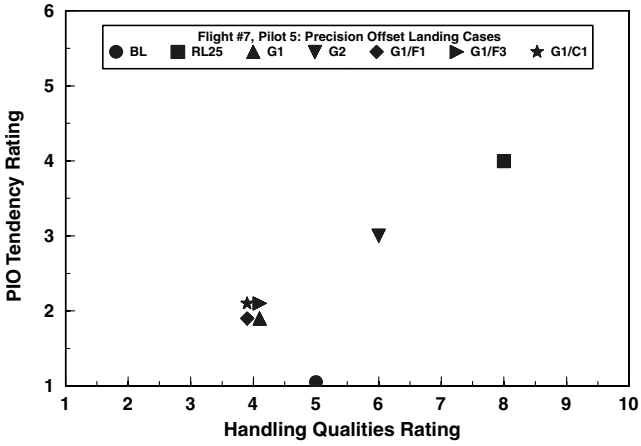

a) Pilot 5

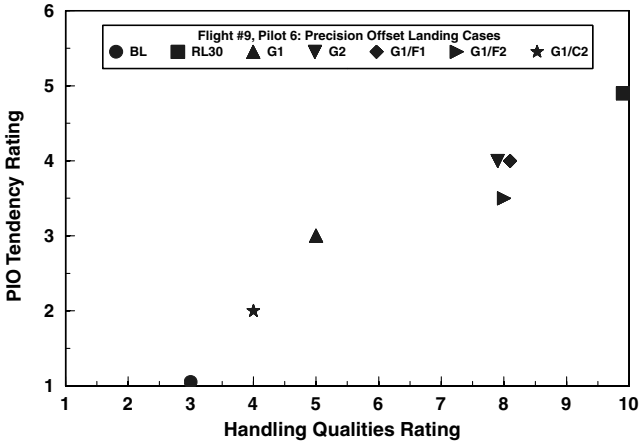

b) Pilot 6

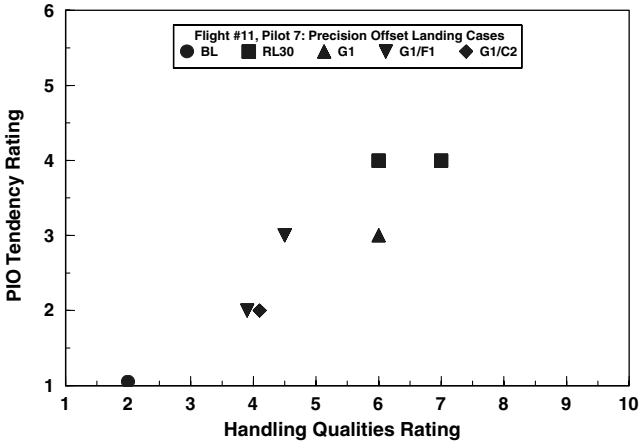

c) Pilot 7

Fig. 9 Pilot ratings for the precision offset landing task.

C. Time Histories

Time history plots for the three precision offset landing example runs are presented in Figs. 10–12 for pilots 5, 6, and 7, respectively. Included in each example are time histories of the pilot's lateral stick input and the bank angle output. For the smart-gain and smart-cue evaluation examples, time histories of the command path smart-gain and the force feedback smart-cue are also given. For pilot 5, there is not a significant difference in the resulting bank angles associated with the large corrections back to the runway centerline with peak angles in the neighborhood of ±20 deg. The differences occur in the final, tightly controlled corrections.

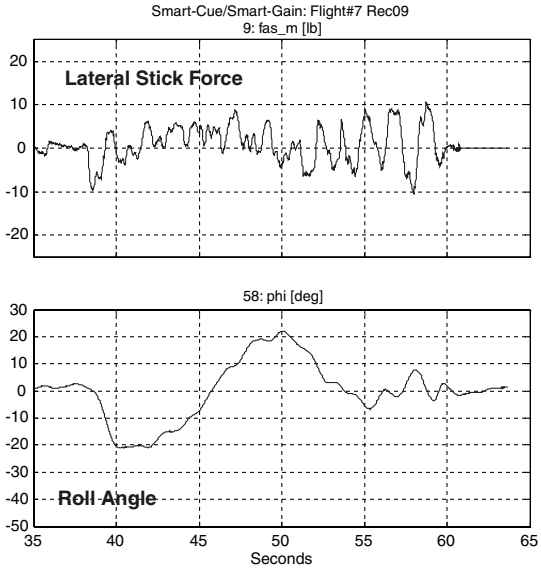

a) RL25 – HQR 8+/PIOR 4

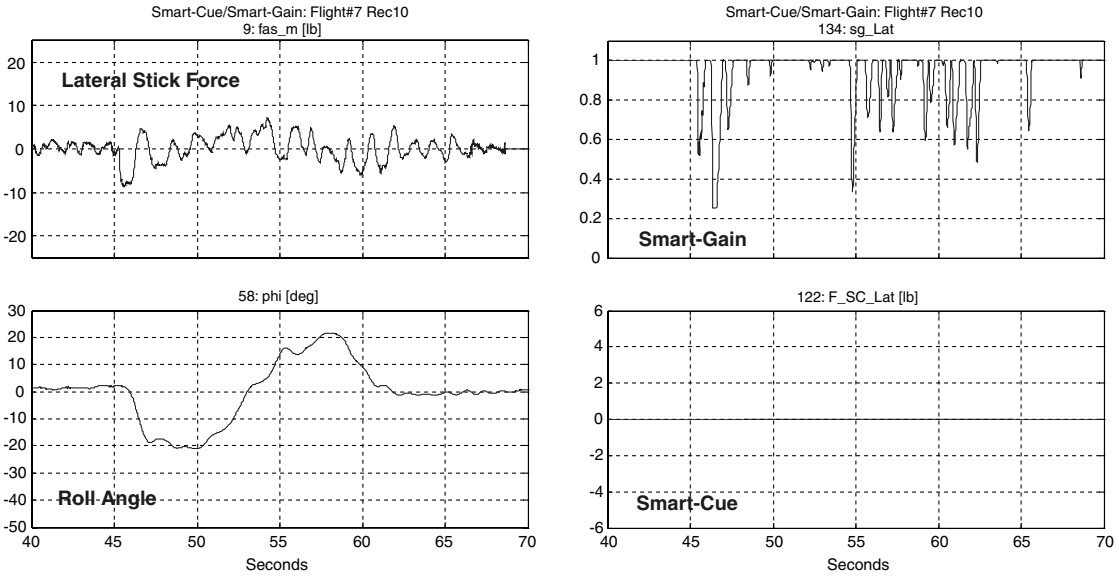

b) RL25, Smart-Gain (G1) – HQR 4/PIOR 2

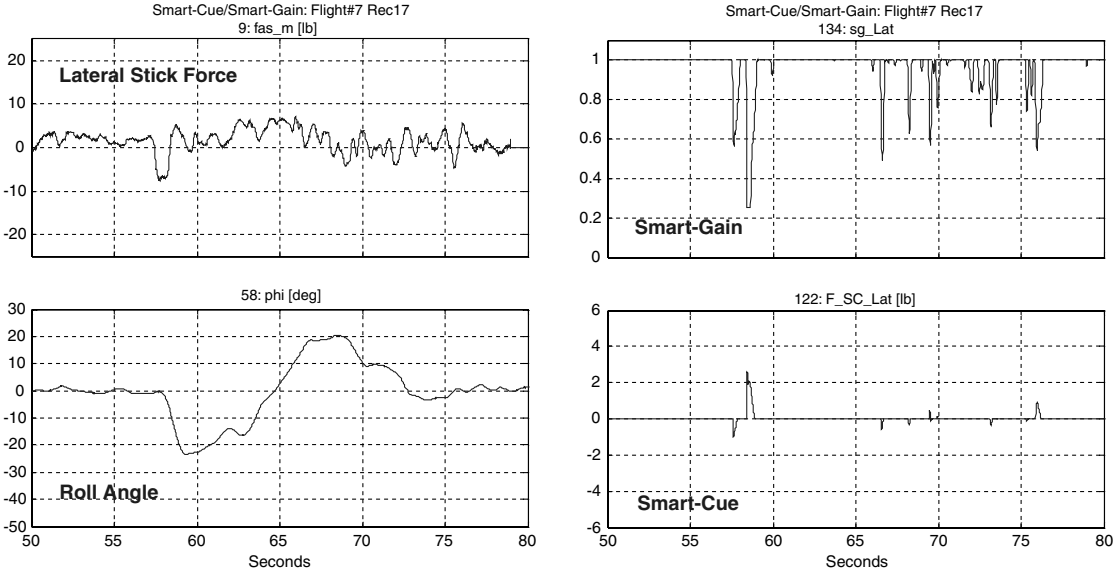

c) RL25, Smart-Cue/Smart-Gain (G1/C1) – HQR 4/PIOR 2

Fig. 10 Time histories for the precision offset landing task, pilot 5.

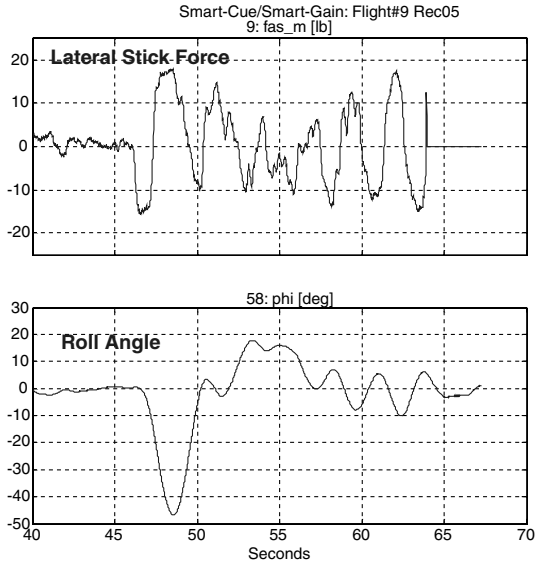

a) RL30 – HQR 10/PIOR 5

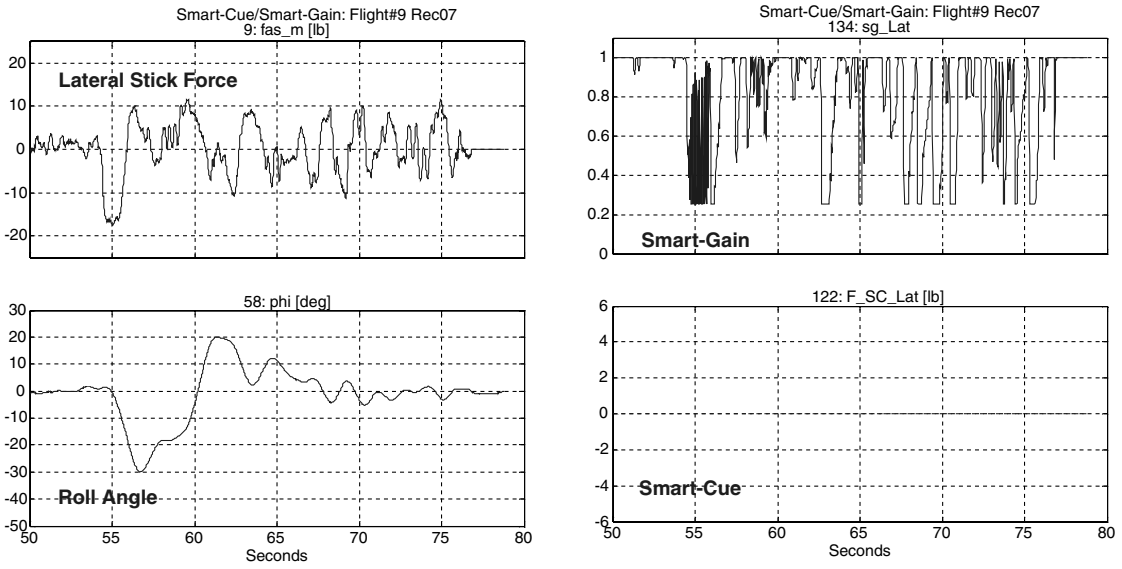

b) RL30, Smart-Gain (G1) – HQR 5/PIOR 3

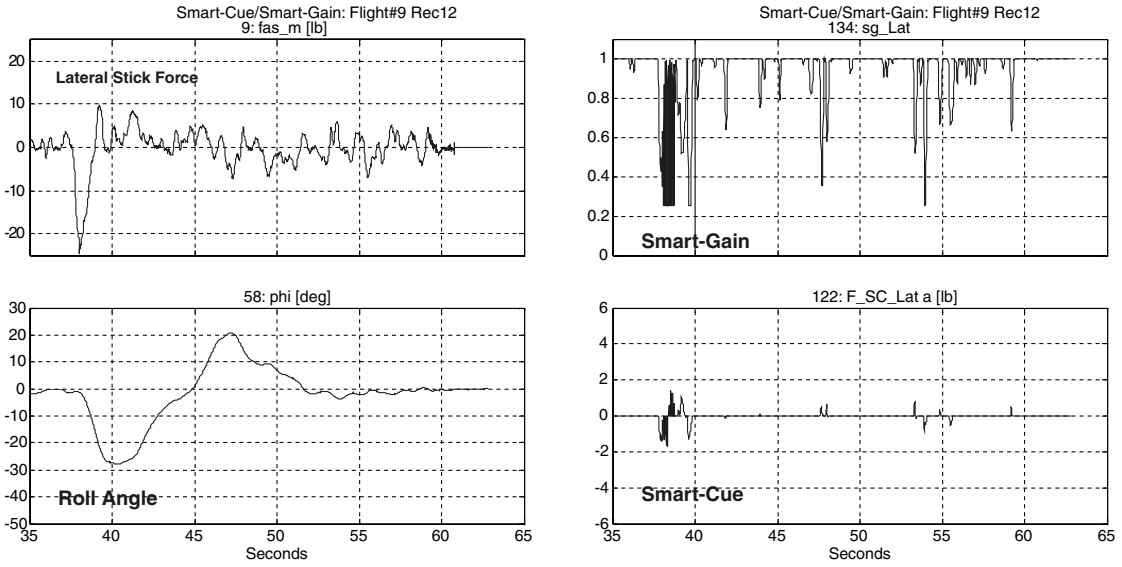

c) RL30, Smart-Cue/Smart-Gain (G1/C2)–HQR 4/PIOR 2

Fig. 11 Time histories for the precision offset landing task, pilot 6.

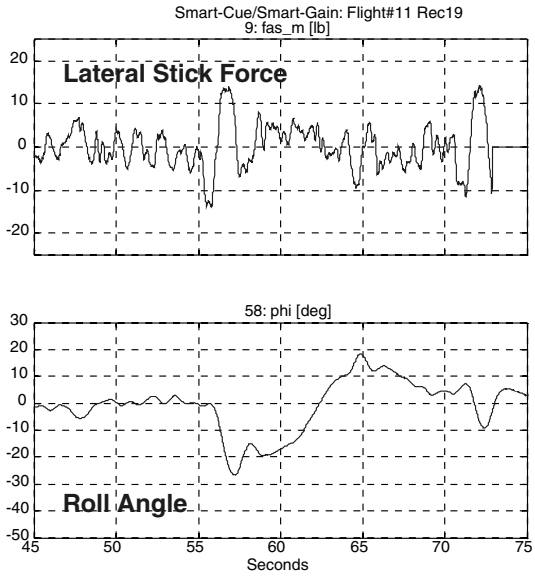

a) RL30 – HQR 7/PIOR 4

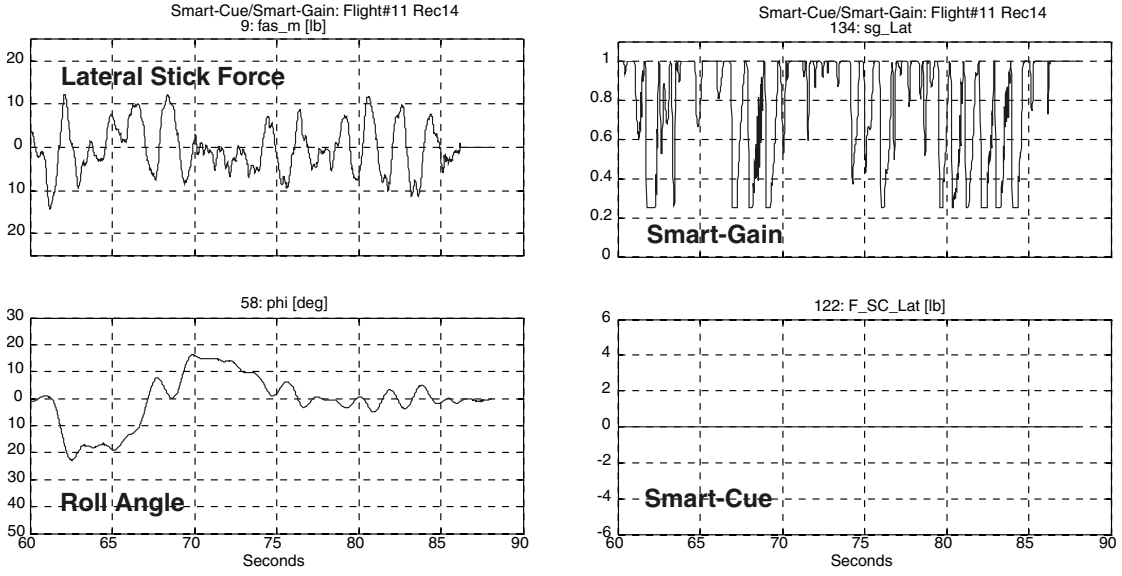

b) RL30, Smart-Gain (G1) – HQR 6/PIOR 3

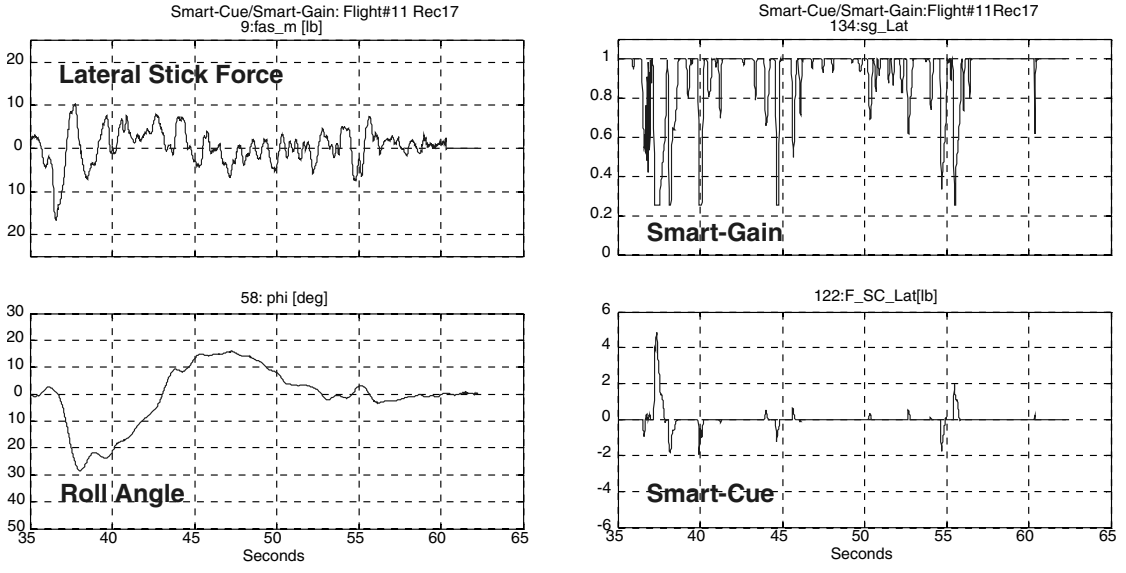

c) RL30, Smart-Cue/Smart-Gain (G1/C2) – HQR 4/PIOR 2

Fig. 12 Time histories for the precision offset landing task, pilot 7.

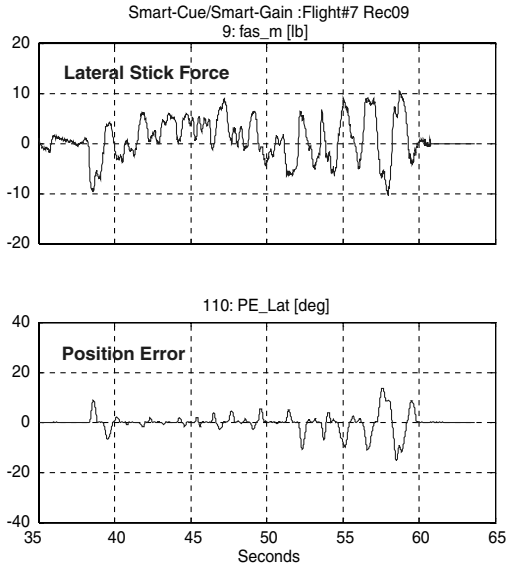

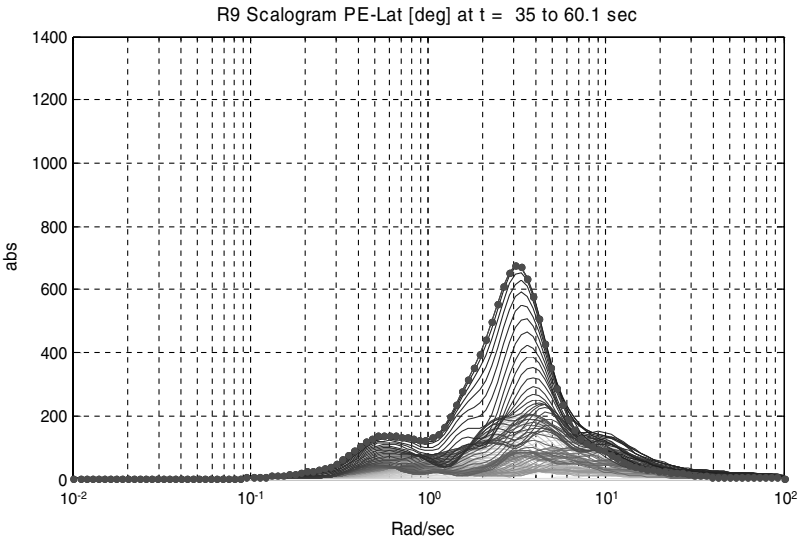

a) RL25 – HQR 8+/PIOR 4

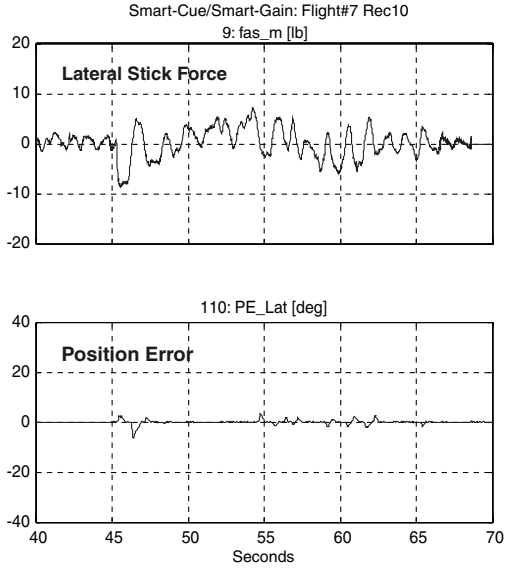

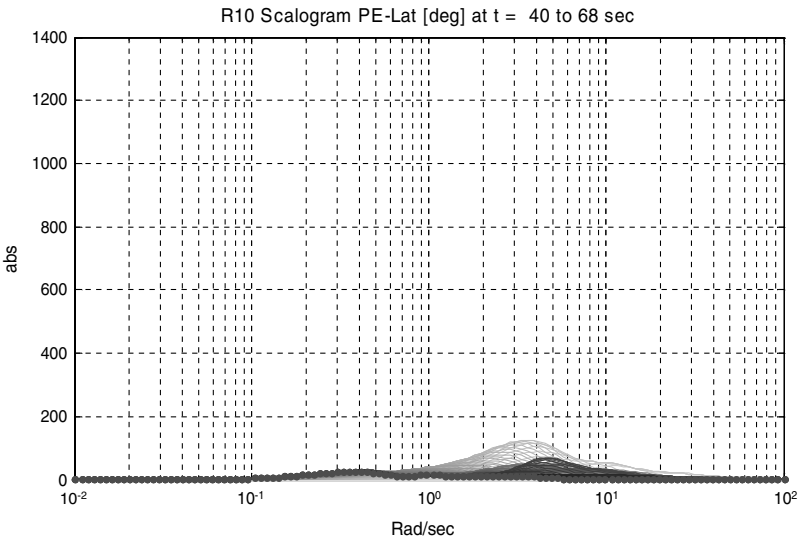

b) RL25, Smart-Gain (G1) – HQR 4/PIOR 2

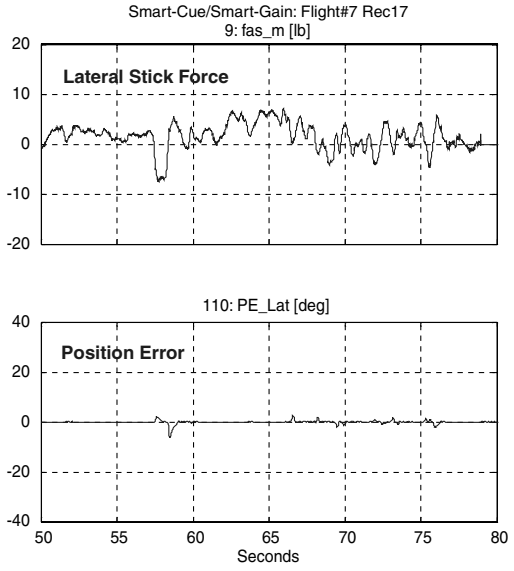

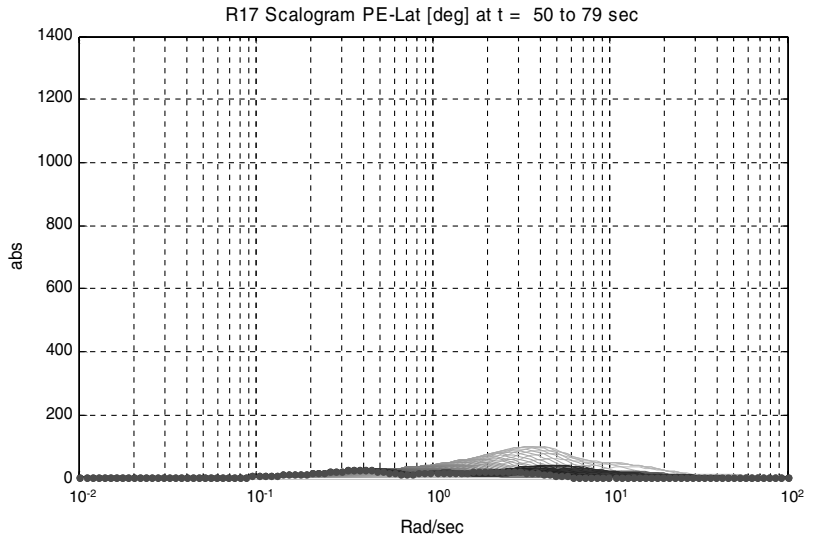

c) RL25, Smart-Cue/Smart-Gain (G1/C1) – HQR 4/PIOR 2

Fig. 13 Lateral position error variations for the precision offset landing task, pilot 5.

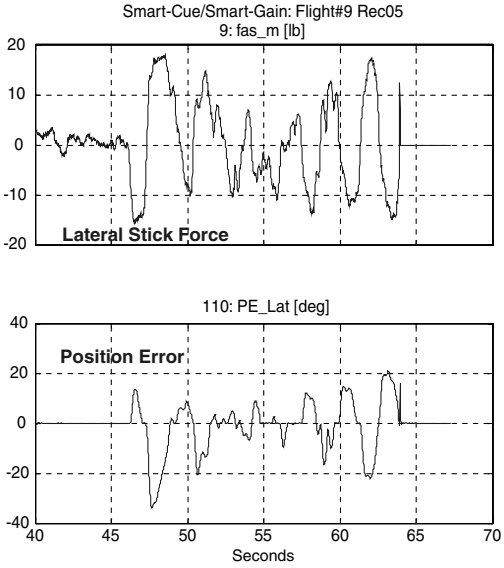

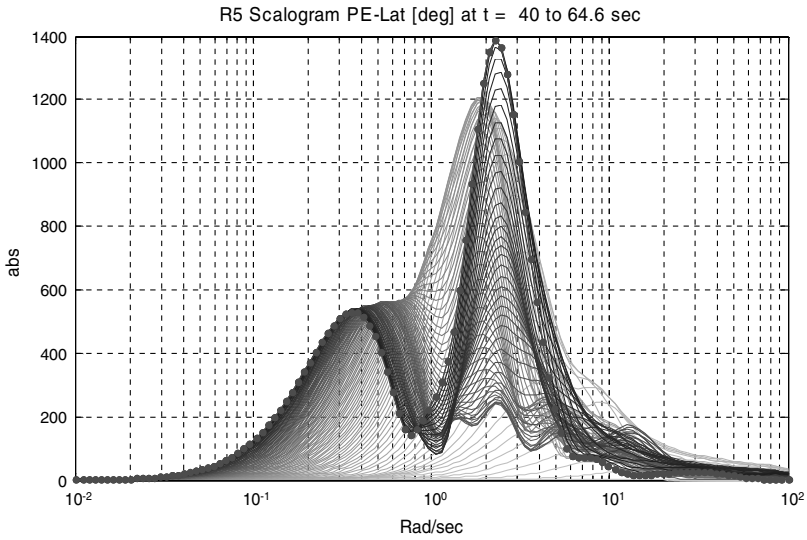

a) RL30 – HQR 10/PIOR 5

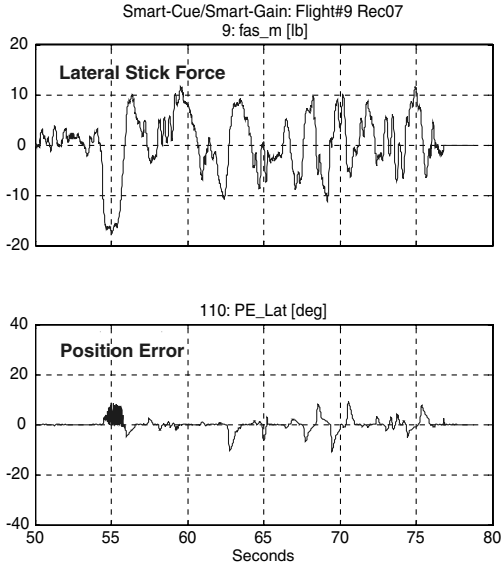

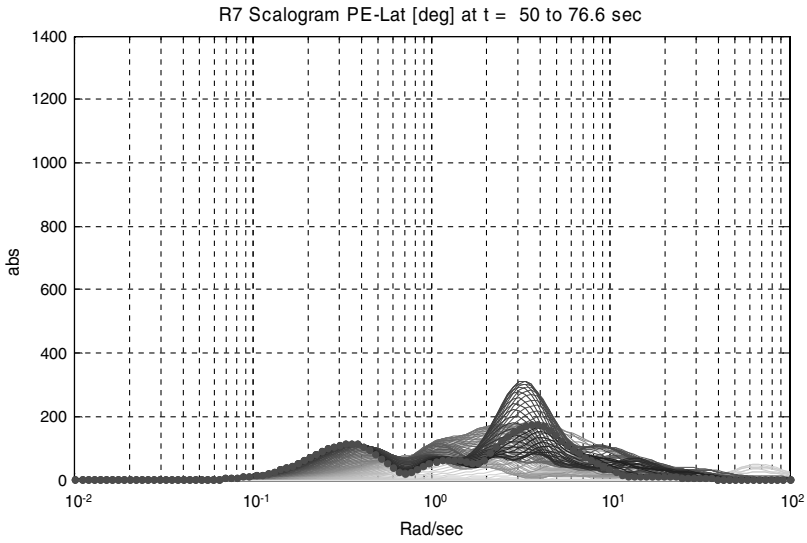

b) RL30, Smart-Gain (G1) – HQR5/PIOR 3

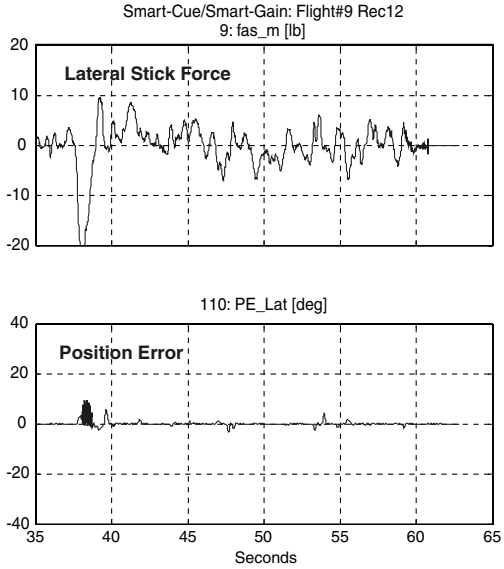

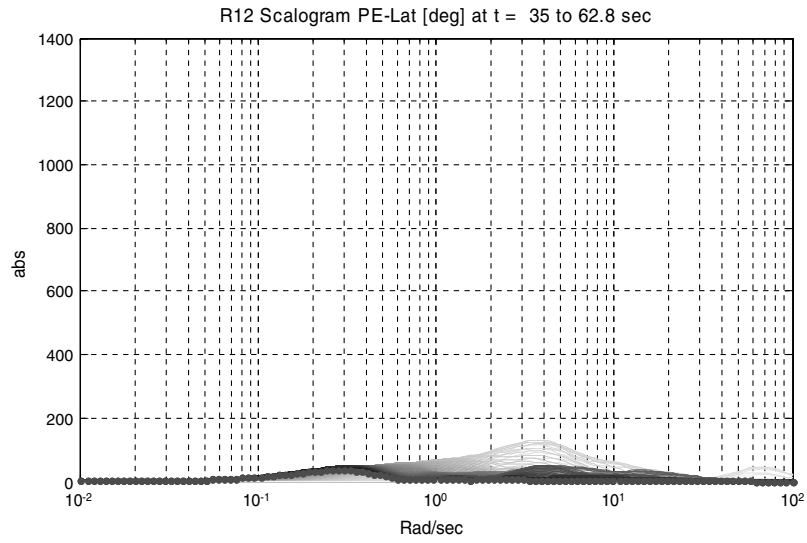

c) RL30, Smart-Cue/Smart-Gain (G1/C2) – HQR4/PIOR 2

Fig. 14 Lateral position error variations for the precision offset landing task, pilot 6.

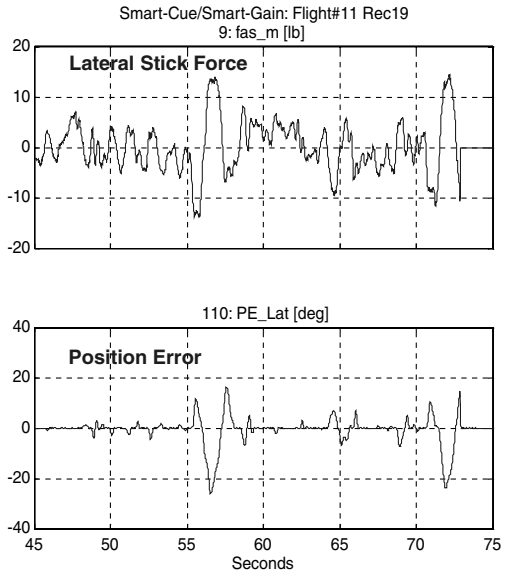

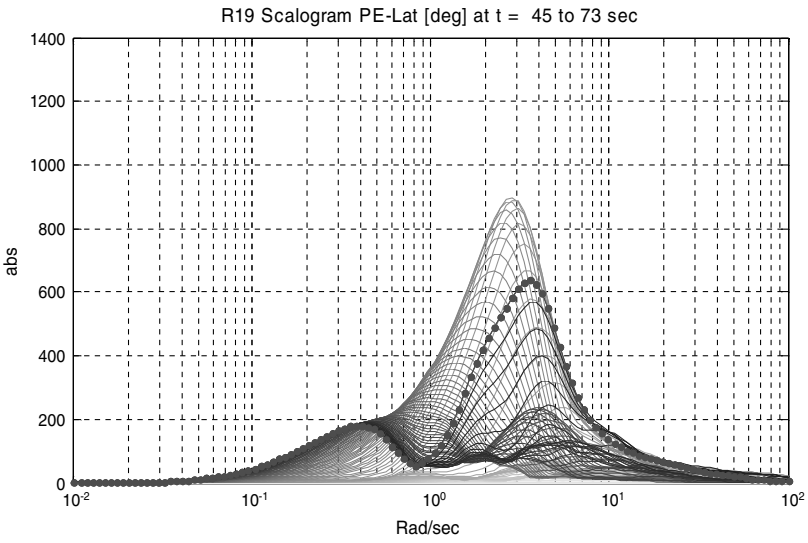

a) RL30 – HQR 7/PIOR 4

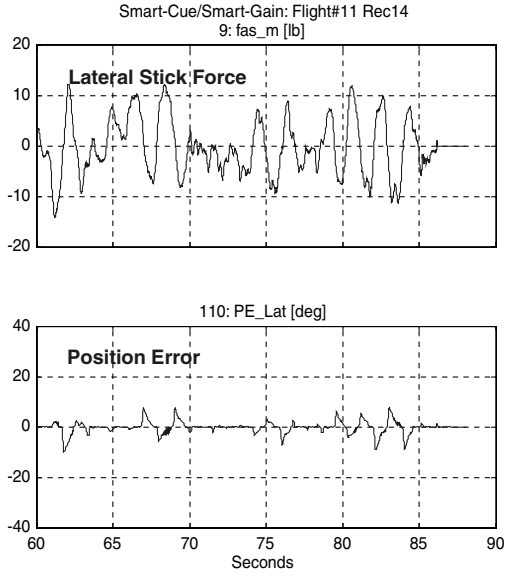

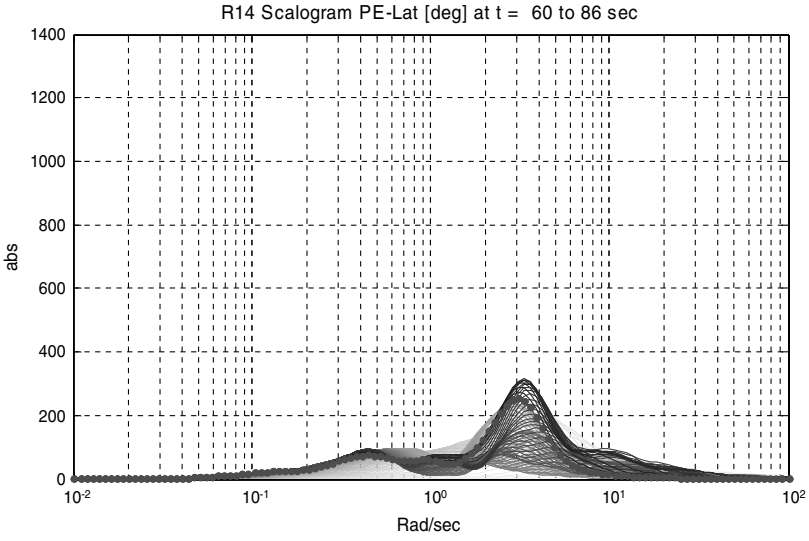

b) RL30, Smart-Gain (G1) – HQR 6/PIOR 3

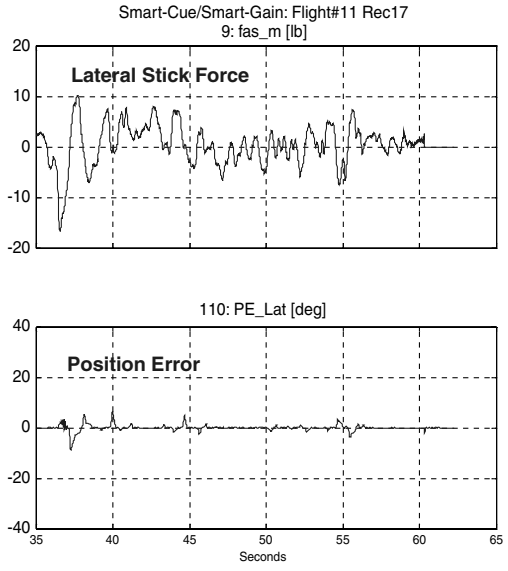

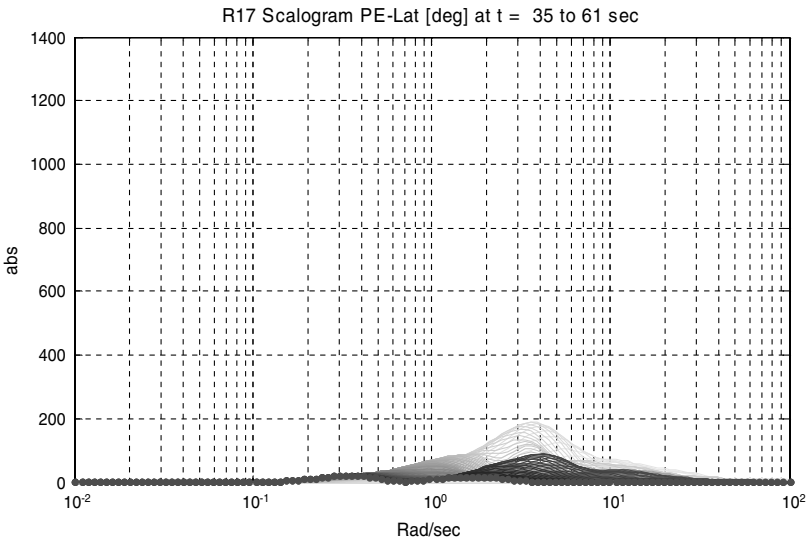

c) RL30, Smart-Cue/Smart-Gain (G1/C2) – HQR 4/PIOR 2

Fig. 15 Lateral position error variations for the precision offset landing task, pilot 7.

Table 3 Pilot ratings and comments for the precision offset landing evaluations

Pilot	Configuration	HQR/PIOR	Pilot comments
5	RL25	8 + /4	I was fully devoted to trying to keep the wings level.
5	RL25 G1	4/2	I felt more connected. There was better predictability.
5	RL25 G1/C1	4/2	Doesn't look terribly different to me.
6	RL30	10/5	It wasn't divergent until I got in the loop.
6	RL30 G1	5/3	There are undesirable motions going on. . . but I am staying on task. I can meet performance, but with considerable compensation.
6	RL30 G1/C2	4/2	That wasn't a problem. That was easy. Performance was good.
7	RL30	7/4	No, I don't like this. As soon as I made the input I realized I wasn't getting what I wanted.
7	RL30 G1	6/3	More controllable, but still hard to make precise inputs. It was not nice right at the end. Probably wouldn't have seen it without the wind.
7	RL30 G1/C2	4/2	I have not felt a cliff where I thought there is a PIO there. Everything felt very controllable without oscillations.

Here, the rate-limited configuration leads to a PIO that resulted in the safety pilot taking control after the third oscillation. Note the increasing amplitude of the oscillatory pilot stick force inputs. No such oscillations are seen in the smart-gain alone and smart-cue/smart-gain configurations. The smart-gain is active whenever the command path gain is not equal to one. Although not necessarily perceived by pilot 5, it is clear that the presence of the smart-cue combined force reduced the amount of smart-gain activity when compared with the smart-gain alone example.

Both pilot 6 and 7 employed a more aggressive technique due to natural tendencies and the presence of moderate turbulence and crosswinds. For pilot 6, the initial correction to the runway centerline resulted in a bank angle of nearly 50 deg, compared to the 20 deg bank angle seen by pilot 5. Furthermore, a divergent PIO resulted from the final corrections and the safety pilot again took control. With the smart-gain and smart-cue active, the resulting bank angle was less than 30 deg and no PIO was observed in the final corrections. The more aggressive technique of pilot 6 resulted in a significantly more active smart-gain reduction. In addition, the smart-gain activity is reduced when used with the combined force smart-cue. For pilot 7, a distinct PIO tendency was observed in the initial correction to the centerline as well as in final corrections. His sensitivity to an impending flying qualities cliff, however, allowed him to avoid sustained oscillations, although the safety pilot did feel compelled to take control at touchdown. The pilot's high level of aggressiveness is further seen in the activity of the smart-gain and in the magnitude of the smart-cue force associated with the initial correction. Once again, the activity of the smart-gain is reduced in the presence of the smart-cue.

D. Position Error Scalograms

The wavelet scalogram [6] not only identifies the peaks in signal power, but also when in time the peaks occurred. It is this characteristic that makes wavelets a powerful tool for detecting changes in time-varying systems and it is this capability that is exploited for identifying from the flight-test data system performance differences with the smart-cue and smart-gain active.

Position error is the measure of dynamic distortion [2]. Thus, if the methods are effective, there should be a significant reduction in position error with the smart-gain and/or smart-cue active. Scalograms offer a unique way to quantify this reduction. Position error scalograms and corresponding lateral stick force and position error time histories for the three precision offset landing example runs are shown in Figs. 13–15 for pilots 5, 6, and 7, respectively. Scalograms, as just described, are essentially time-varying power spectra density plots that not only show at what frequencies the peak power is occurring, but also at what point in time. Approximately 30 s of data that have been selected to capture the heart of the offset landing are included in the plots shown here, with the most current time slice displayed as a series of dots. Then, as time moves back to the earliest interval displayed on the plot, the solid "lines of persistence" change from dark to light. Note that the same plot scales are used for all of the plots, so that both intra- and interpilot variations can be easily studied. The absolute power units for the scalogram of position error are $\mathrm{deg}^2/(\mathrm{rad/s})$.

Because the position error is tied closely to the control activity of the pilot, the position error power occurs predominantly in the frequency range associated with pilot control (i.e., 0.1–20 rad/s). For the pilot 5 example cases, the peak power occurs during the PIO associated with the final correction of the rate-limited example (see Fig. 13a). In this case, the peak power closely correlates with the observed PIO frequency of 3.4 rad/s. With the smart-gain and smart-cue active, the peak power is reduced by approximately a factor of 6. As noted previously, the smart-gain alone does much of the work for pilot 5, although some further improvements are seen with the smart-cue active as well.

Comparing interpilot results, the largest peak in position error power was seen in the pilot 6 rate-limited example case of Fig. 14a. This peak is associated with the divergent PIO that developed during the final corrections, which was discussed earlier. For this pilot, the addition of the smart-gain produces a reduction in position error power by a factor of 4.5, however, the smart-gain plus smart-cue results in a reduction by a factor of nearly 14. Although not as dramatic, similar trends are seen in the pilot 7 results of Fig. 15. For both pilots 6 and 7, the combination of smart-gain and smart-cue was required to achieve the best results.

VI. Conclusions

Approach and landing flights were conducted with three evaluation pilots using the Calspan Learjet II in-flight simulator. All of the approach and landing evaluations were made at Niagara Falls Airport. The crew for the checkout and evaluation flights consisted of a Calspan safety pilot, an evaluation pilot, a Calspan flight-test engineer, and the Systems Technology, Inc. flight-test conductor. Conclusions from the approach and landing flight tests are as follows:

1) For the roll axis approach and landing evaluations, the clear performance enhancer for all three pilots was the smart-gain. In the checkout flights, it was difficult to achieve adequate landing performance with the rate-limited configuration using the smart-cue alone.

2) Addition of the smart-cue, however, was an important performance benefit for two of the three pilots. For these pilots, the evaluation flights took place on a day with significant crosswinds and turbulent air that resulted in added work load for the precision offset landing task. The same smart-gain and combined force smart-cue produced the best results for both pilots. This combination consistently gave desired performance with no pilot-induced oscillation tendencies over repeated evaluations, which was significant considering that the wind conditions varied from run to run.

3) The third pilot flew on a calm air day, which allowed him to use smoother pilot inputs associated with his lower gain technique. In this environment, the smart-gain alone did much of the work and only small smart-cue forces that may have been imperceptible to the pilot were ever present.

When used together, the smart-gain and smart-cue were found to enhance flight safety in the approach and landing task by significantly reducing pilot–vehicle-system loss of control incidents that routinely occurred with the rate-limited-alone configuration.

Acknowledgments

The work described herein was conducted as part of a Phase II Small Business Innovation Research program sponsored by NASA Dryden Flight Research Center. The authors would like to acknowledge Timothy Cox of NASA who served as the NASA technical representative and Ralph A'Harrah of NASA Headquarters (retired) who provided the "call to action" and technical review for the work described herein. The authors also acknowledge all of those at Calspan Flight Research that participated in the flight-test program, including Paul Schifferle, manager of Calspan Flight Research, Ryan McMahon, flight-test engineer, and test pilots Paul Deppe, Russ Easter, Dave Culbertson, Lou Knotts, and Kevin Prosser. Furthermore, the authors acknowledge the participation of Boeing Commercial Airplanes with special recognition for Brian Lee and test pilot Mark Feuerstein. The work conducted on this program is dedicated to Duane McRuer who passed away in January 2007. His technical expertise inspired the advances made in this program. He will be greatly missed.

References

[1] Klyde, D. H., and Mitchell, D. G., "Investigating the Role of Rate Limiting in Pilot-Induced Oscillations," *Journal of Guidance, Control, and Dynamics*, Vol. 27, No. 5, Sept.–Oct. 2004, pp. 804–813. doi:10.2514/1.3215

[2] Klyde, D. H., and McRuer, D., "Development of Smart-Cue and Smart-Gain Concepts to Alleviate Pilot-Vehicle System Loss of Control," AIAA Paper 2008-6209, Aug. 2008.

[3] Klyde, D. H., Bachelder, E. N., McMahon, R., Weingarten, N. C., and Harris, C., "Use of In-Flight Simulation to Create a Flying Qualities Database," AIAA Paper 2008-1624, Feb. 2008.

[4] Cooper, G. E., and Harper, R. P., Jr., "The Use of Pilot Rating in the Evaluation of Aircraft Handling Qualities," AGARD Rept. 567, April 1969.

[5] Weingarten, N. C., and Chalk, C. R., "In-Flight Investigation of Large Airplane Flying Qualities for Approach and Landing," U.S. Air Force Wright Aeronautical Labs TR-81-3118, Sept. 1981.

[6] Thompson, P. M., Klyde, D. H., Bachelder, E. N., and Rosenthal, T. J., "Development of Wavelet-Based Techniques for Detecting Loss of Control," AIAA Paper 2004-5064, Aug. 2004.

[7] Deppe, P. R., Chalk, C. R., and Shafer, M. F., "Flight Evaluation of an Aircraft with Side and Center Stick Controllers and Rate-Limited Ailerons," NASA CR-198055, Nov. 1996.